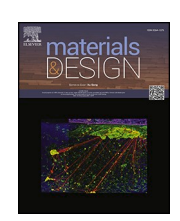
ELSEVIER

Contents lists available at ScienceDirect

Materials & Design

journal homepage: www.elsevier.com/locate/matdes





Electrical characterization of thermal vacuum grown submicron-thick Sn whiskers

Agata Skwarek^a, Balázs Illés^{a,b,*}, Ernest Brzozowski^c, Adam Łaszcz^c, Piotr Zachariasz^b

- ^a Łukasiewicz Research Network, Institute of Microelectronics and Photonics, LTCC Research Group, Kraków, Poland
- b Budapest University of Technology and Economics, Faculty of Electrical Engineering and Informatics, Department of Electronics Technology, Budapest, Hungary
- ^c Łukasiewicz Research Network, Institute of Microelectronics and Photonics, Materials Characterization Research Group, Warsaw, Poland

ARTICLE INFO

Keywords: Sn whisker High vacuum Space environment Reliability Breakdown voltage Current capacity

ABSTRACT

Submicron-thick Sn whiskers were electrically characterized. The whiskers were grown from a 500 nm thick Sn layer on a Cu substrate, which was kept in a thermal vacuum chamber ($50\,^{\circ}$ C and 8.3×10^{-6} mbar for 1000 h) to simulate the space circumstances. First, the electrical parameters were measured in ambient conditions by welding the whisker to a sample holder. Next, a real circumstance was simulated when whiskers touched a conductive surface using a probing method in a vacuum. The average breakdown voltage was 10– $12\,$ V. Two types of I-V characteristics of the whisker were observed: an abrupt breakdown in the case of needle-type whiskers and a slower breakdown in the case of nodule-type whiskers. Nodule-type whiskers had a relatively larger current capacity than needle-type whiskers. TEM investigations showed that both whisker types were mono-crystalline, but the nodule-type whiskers were more oxidized and contained more Cu/Cu₆Sn₅ inclusions than the needle-type whiskers, which explains the electrical differences. In ambient conditions, a whisker can conduct more than three times larger current (over $100\,$ mA) than in vacuum due to the thermal management effect of the ambient air. The space industry can use the obtained electrical parameters for risk analyses and the development of short-circuit protection systems.

1. Introduction

The RoHS directive, containing lead-free changes, had a great impact on the microelectronics industry in 2006. Entirely new materials, like solder alloys, surface coatings, fluxes, etc., have started to be applied to produce commercial electronic devices. The space sector was and still is not under the direct constraint of RoHs, although they cannot avoid the RoHs-induced market changes, which can cause risks for them. The transition to lead-free technology resulted in a reduced market availability for lead-containing soldering materials. Thus, the space industry needs to use printed circuit boards (PCBs) and components with leadfree surface finishes, which can have compatibility problems with lead-containing solder alloys [1]. Therefore, the space sector has also been interested in lead-free technology. In 2012, the European Space Agency (ESA) published guidelines about their lead-free control plan and evaluated the lead-free risks in the space sector [2]. In 2020, they published the roadmap and authorization plan for lead-free transition [3,4], marking the earliest date to 2026 [4].

ESA has been putting a lot of effort into researching the risk of leadfree electronics used in space environments and has identified that one of the main risks is Sn whisker growth [4]. Sn whiskers are conductive Sn filaments, which can grow from pure or high Sn-content objects (like solder joints and component terminals) as a result of different mechanical stresses acting on the given object. The Sn whisker grows as a mechanical stress relaxation mechanism of the Sn object. This mechanical stress can be a direct mechanical load, built-in residual stress of the Sn layer, volumetric change induced stress (like oxidation or intermetallic formation), and thermomechanical stress (due to CTE differences) [5]. Sn whiskers can cause considerable reliability problems, mostly by short circuit formation between the terminals of the components (not exclusively) since their length can exceed the millimeter dimension. At least six satellites (GALAXY IIIR, GALAXY IV, GALAXY VII, SOLIDARIDAD, OPTUS B1, and DBS-1) have been totally or partially lost due to an approved Sn whisker phenomenon so far. In addition, the first malfunction usually appeared relatively early, in ~5 years, and total loss occurred in 5-10 years.

E-mail address: illes.balazs@vik.bme.hu (B. Illés).

^{*} Corresponding author at: Budapest University of Technology and Economics, Faculty of Electrical Engineering and Informatics, Department of Electronics Technology, Budapest, Hungary.

The literature on the Sn whiskers is very wide; however, the studies with space (vacuum) conditions are less representative. Two independent sources [6,7] reported that Sn whiskers could cause electronic malfunctions on spacecraft by vacuum metal arcing. Umalas et al. [8] found that not only Sn but also Ag can produce electron beam-induced whiskers in a vacuum chamber during scanning electron microscopy (SEM). Brusse et al. [9,10] shown that Sn whiskers can be even more dangerous in space (vacuum) than in ambient conditions since they can cause not only short circuits but further defects: they can interfere with optical surfaces; they can be fused by the current heating and the vaporized Sn can form a plasma that can conduct more even more current than the whisker itself. Sn whiskers grown from Sn-plated relays caused the complete losses of satellites (Galaxy IV, Galaxy VII, Solidaridad I) by Sn vapour arc in a vacuum [9].

Williams et al. [11] observed Sn hillock growth during in-situ indentations in an SEM device under a vacuum (1.3 \times 10⁻⁴ Pa). They found that hillock grew linearly over time when the stress was relieved slowly, and a sigmoidal-type (arresting growth) occurred when stress was relieved quickly. Moon et al. [12] kept a bright Sn-Cu electrodeposited film in the chamber of an Auger system at 2×10^{-9} Pa for 9 days. They cleaned a part of the sample from the oxides using an Ar⁺ ion beam, and they found Sn whiskers on both parts of the sample but longer ones on the oxidized part. Barsoum et al. [13] found that the Sn surface kept in ambient circumstances produced considerably more amount and longer whiskers than the same Sn surface kept in a vacuum. Suganuma et al. [14] observed partially opposite results during a thermal cycling $(-40-125 \,^{\circ}\text{C})$ test of Sn films on ceramic substrates in vacuum (10^{-4}Pa) and ambient conditions. The samples in the vacuum produced thinner and longer whiskers, but their number was not affected by the atmosphere. The same results were published by Ichimaru et al. [15] in the case of pure Sn platings on Ni/Cu and Alloy42 substrates. Jo et al. [16] compared the Sn whisker susceptibility of matt Sn electroplating also by thermal cycling ($-20 \text{ to } 80^{\circ}\text{C}$) in air and in vacuum (10^{-4} Pa). They observed more intensive whisker growth and thinner whiskers in a vacuum than in air. Oudat et al. [17] demonstrated the electrostatic nature of the whisker growth; thus, they observed whiskers grew from Sn thin film on a glass substrate in a vacuum by x-ray and gamma-ray irradiation. Liu et al. [18] found rapid Sn whisker growth from Ti₂SnC-Sn samples in room conditions and in vacuum, as well.

Even though the electric properties of the Sn whisker cause the problem, we know much less about it than about its growth properties. The failure modes caused by tin whiskers can be grouped into four different categories: permanent short circuits in low-current applications, transient short circuits in applications where the current is high enough to cause the whisker to fuse open, metal vapor arcing in a vacuum, and debris/contamination resulting from vibration, which frees loose whiskers that can interfere with optical surfaces or bridge exposed electrical conductors [9]. Han et al. [19] proposed a measurement system where whiskers placed on the card rail are contacted with two kinds of plated tungsten probes, i.e., Au and Sn. They found that even if the whisker bridged two metal paths, an electrical short was not guaranteed. There is a threshold voltage (breakdown voltage) that must be exceeded in order to produce current flow due to weak physical contact between whiskers/paths and the presence of non-conductive surface tin, which can be an oxide layer. This voltage level is the level of the transition to metallic conduction current, where the film and oxide layers break down [20]. Han et al. [19] measured breakdown voltage in the range 0 to 43.85 V, and the mean was 7.57 V.

Courey et al. [20,21] investigated the contact resistance between the measurement probe and whisker during the electrical characterization of Sn whiskers. They found that it contains not only the oxide film resistance but the constriction resistance as well, which originated from the roughness of the whisker surface. It was theoretically calculated that the film resistance is significantly higher than the constriction resistance. Furthermore, the whiskers can bend when they are touched. Courey et al. [20,21] measured breakdown voltages between 3 and 44 V.

The current data showed single, multiple, and multiple transitions with intermittent contact between 2 and 3 mA.

Generally, in the literature, there are only a few old references related to the current that a whisker can carry. Sabbagh and McQueen [22] reported that the burning-out current for a 3 mm long whisker was 10 mA. The diameter of the whisker was not reported. Hada et al. [23] measured the current carrying capacity to be 10 mA for whiskers with a 1 μm diameter, up to 30 mA for whiskers with a 2.5 μm diameter, and up to 75 mA for whiskers with a 4 μm diameter. Dunn [24] reported a fusing current of 10 mA for a 1.1 μm diameter whisker, 20 mA for a 1.5 μm diameter whisker, and the highest reading in his study was 32 mA for a 3 μm whisker. They also measured the electrical resistivity of Sn whiskers and found that it is close to the resistivity of Sn (11.3 $\mu \Omega$ cm) if the whisker is thin, but it can reach even 59 $\mu \Omega$ cm if the whisker is thicker. The difference was attributed to possible internal defects in the thicker whiskers' bodies. Panashchenko [25] modelled the fusion current of different metal whiskers in a vacuum:

$$I_f = \left(\frac{2\sqrt{L_z}T_0}{R_0}\right)\cos^{-1}\left(\frac{T_0}{T_f}\right) \tag{1}$$

where R_0 is the ohmic resistance of the whisker, L_z is the Lorenz number, T_0 is the ambient temperature, T_f is the fusion temperature. They found that the fusion current of Sn whiskers is 87.5 mV/ R_0 . Brusse et al. [9] measured that thicker whiskers can conduct even 50 mA without fusion.

Some studies investigated the secondary effect of whisker fusion in a vacuum, which is the formation of plasma. Mason and Eng [26] found that, with over 18 V of supply, the whiskers could fuse and vaporize, which initiates a plasma that can conduct more than 200A. They could produce stable Sn plasma from whiskers in a vacuum at power supply voltages 4 V, which means a considerable risk for electronic devices in a space environment since this voltage level is lower than the 5.5 V voltage commonly used for transistors and logic circuits. In addition, they observed that both the breakdown voltage and the plasma shutoff were accompanied by voltage spikes that exceeded the applied DC voltage, which might mean that Sn whisker plasma is even more dangerous on circuits that are sensitive to transients.

Consequently, Sn whisker-caused failures mean considerable reliability risk in space-used electronic devices, and it can just grow with the change to lead-free in the space industry. The Sn whisker growth phenomenon: different inducing factors, the microstructure of the different whiskers, whisker susceptibility of the different Sn alloys, are much more researched than the short circuit formation ability (electrical parameters) of the Sn whiskers. In our work, we developed submicronthick Sn whiskers from Sn thin films on Cu substrates in thermal vacuum conditions and characterized their breakdown voltage and current capacity by two different measurement methods.

2. Materials and methods

2.1. Sample and whisker preparation

Pure Cu sheets were prepared using the cold sheet rolling method. Substrates were punched from the sheets to 9 cm² size. The Cu substrates were relaxed from residual stresses by heat-annealed at 150 °C for 2 h. The cleaning process was executed by chemical degreasing using a Uniclean 251 solution (Atotech) at 48 °C for 5 mins, followed by chemical oxide removal using 10 % $\rm H_2SO_4$ solution for 1 min. Physical vapour deposition (PVD) was applied to cover the substrates with pure (99.99 %) Sn in an evaporator (BALZERS BA 510). Before the evaporation, the ion bombardment was used to neutralize the surface of the substrates in the evaporator. The evaporator worked with a resistive evaporation technique using a Wolfram boat, which was heated up with 2.5 kV/9A in a vacuum (10 $^{-4}$ Pa). The evaporation time was 10 s. The thickness of the Sn layer was between 400 and 500 nm, measured by an Alpha-Step 500 surface profiler. The samples were kept in an 8.3×10^{-6}

mbar vacuum at 50 $^{\circ}$ C temperature for 1000 h. After the thermal vacuum test, the surface of the samples was investigated by a Helios Nanolab 600 dual-beam scanning electron microscope (SEM)/ focused ion beam (FIB) to sort and select the developed whiskers for electrical characterization.

2.2. Electrical characterization of the whiskers

Two methods were applied to characterize the breakdown voltage and current capacity of the Sn whiskers. The first method is based on the removal of the whiskers from their position, welding them on a prepared sample holder, and measuring them under ambient conditions (referred to as the welding method). The second method is based on the classical probing method, which is when the whiskers are contacted by a micromanipulator in the vacuum chamber of the SEM device (referred to as the probing method).

For the welding method, sample holders have been prepared on 4-inch $\mathrm{Si/SiO_2}$ wafers by photolithography. The sample holders had contact pad matrix shapes with different gap distances between 10 and 100 μm , to handle whiskers with different lengths (Fig. 1a). The preparation of the whiskers for the electrical characterization with the welding method contains the following steps (Fig. 2b):

- The FIB manipulator needle is welded to the chosen whisker using deposition techniques in FIB by local metal deposition.
- 2. The whisker is broken off, removed from the Sn layer, and transported to the sample holder.

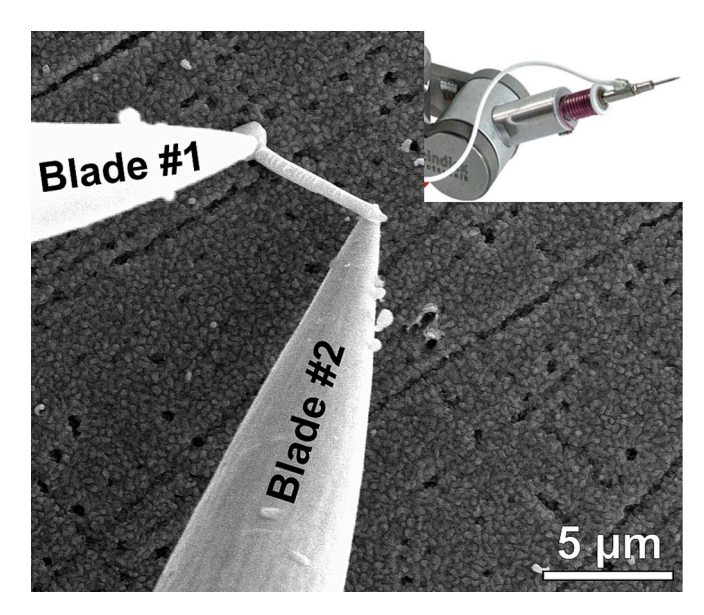


Fig. 2. Electrical characterization of Sn whiskers by the probing method.

3. The ends of the whisker are welded to the contact pads of the sample holder, and the manipulator needle is separated from the whisker.

It has to be noted that with the welding method, only needle-type whiskers could be measured, since the whisker must lie parallel to the

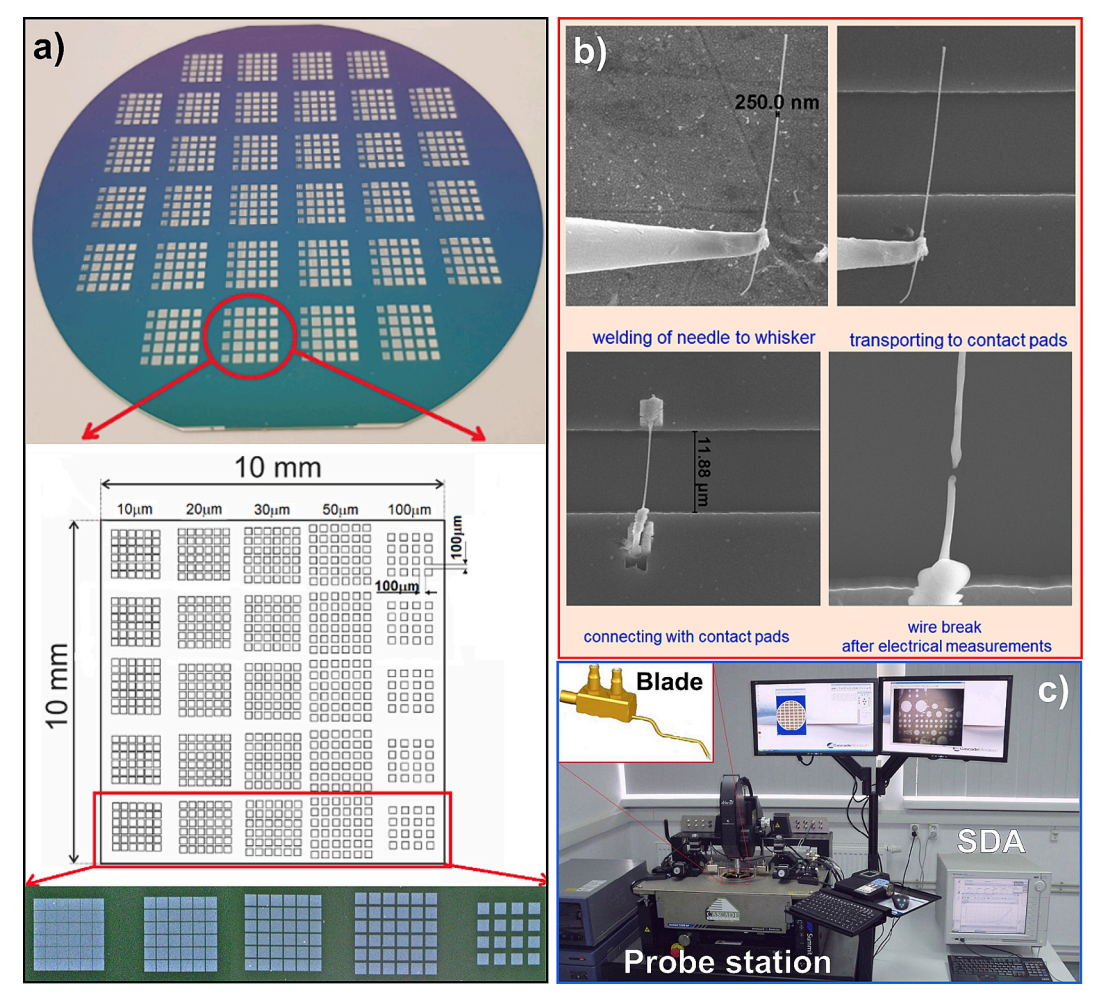


Fig. 1. Electrical characterization of Sn whiskers by welding method: a) sample holder; b) whisker preparation steps; c) probe station.

two contact surfaces of the sample holder to be able to weld them well. In the case of twisted nodule-type whiskers, this condition could not be fulfilled.

After the preparation of the whiskers, the sample holders were placed into a probe station (CASCADE SUMMIT), and their testing blades (Fig. 1c) were connected to a semiconductor device analyzer (SDA) (KEYSIGHT B1500) by TRX cables. The device analyzer has a source-measurements unit (SMU) that can be operated as a voltage or current source and a voltage or current meter. In our setting, the SMU was operated as a voltage source current meter. I-V characteristics were measured with a 500 μs time step. The electrical measurements were performed outside the vacuum chamber of the SEM/FIB device, in ambient conditions. It has to be noted that with the welding method, only the longer needle-type whiskers (Fig. 1b) could be measured.

During the probing method, the whiskers were electrically characterized in the vacuum chamber of the SEM/FIB device, under 4×10^{-6} mbar pressure. The whiskers were contacted with a micromanipulator (KLEINDIEK) having tungsten blades: Blade #1 of the micromanipulator touched the surface at the root of the whisker, and Blade #2 touched the end of the whisker (Fig. 2). Blade #1 penetrated/scratched the surface, resulting in proper electrical contact. At the end of the whisker, the oxide layer needed to be broken first by a sufficiently high voltage to allow the current to flow. The micromanipulator was connected to the same SDA unit, and the same settings were applied as during the welding method.

2.3. TEM measurements

Some whiskers have been selected for transmission electron microscopy (TEM) investigations. TEM lamellae were prepared from the whiskers by a Thermo Scientific Scios 2 – focused ion beam (FIB), using Ga^+ ions for the milling. The surface of the whiskers was covered with a Pt layer before ion milling to protect them from damage caused by the high-energy Ga ions. The samples were transferred to Cu support grids. The lamellae were investigated by a Thermo Fisher THEMIS 200 aberration-corrected TEM/STEM. Spectrum imaging using scanning TEM (STEM) and energy dispersive x-ray spectroscopy (EDS) analysis was executed to define the elemental composition of the samples. The crystallographic structure of the Sn whiskers was determined by the selected area electron diffraction (SAED) technique.

3. Results and discussions

The thermal vacuum test developed Sn whiskers after 75 h of the PVD layer deposition. Fig. 3 presents the typical whiskers, which were detected on the surface of the PVD Sn layer. All whisker types, hillock, nodule, and filament, were detected. The Sn whisker growth was statistically evaluated previously [27], and it was found that, after 500 h, the whisker density reached 60 pcs./10E4 µm². The most frequent length was short, 1.2-1.4 µm, which means that mostly short whiskers grew. The longest detected whisker was 139.1 µm [27]. Some tens of whiskers longer than 50 µm were detected, which could be dangerous for fine-pitch microelectronics. Usually, the end part of the whiskers had a block-like structure with a totally plain surface (Fig. 3a, and d), while at the root of the whiskers, they had a twisted body with grooves (like the usual whisker morphology, Fig. 3b and d). Previously, it was proven that the block-like part grew first in the vacuum, and later the twisted part in the ambient conditions when the samples were waiting for evaluation. The block-like structure and the plain surface were caused mostly by the lack of oxidation in the vacuum chamber [27].

Fig. 4 presents the electrical characteristics of Sn whiskers measured by the welding method. The whiskers were named W1-W3, and their physical appearance is presented in Fig. 4b. The ohmic characteristic of the whiskers is typically visible; the current monotonously increases with the voltage till the whisker fuses (Fig. 4a). The measured whiskers have a diameter between 250–320 nm and large current capacities (3–3.8 mA) measured in the ambient atmosphere. Whisker W1 and W3 showed very similar current–voltage (I-V) diagrams; the current increased fast till \sim 0.4–0.5 V, and later, it slowed considerably until the whiskers fused around 14–16 V. Whisker W2 was different; it presented a nearly linear I-V diagram and fused much earlier (\sim 7V), but it could conduct the highest current. It is worth investigating the resistance–voltage (R-V) characteristics to understand more about what happens during the welded measurement method (Fig. 4c and d).

Generally, all investigated whiskers showed nearly linear R-V characteristics, which was expected in the investigated temperature range, $20\text{--}400\,^{\circ}\text{C}$, according to the literature [28,29]. It was proven before that the whiskers can contain a considerable (4–12 wt%) amount of Cu taken from the Cu₆Sn₅ intermetallic layer between the Cu substrate and the Sn layer [27]. So the specific electric resistance of the whisker could be closer to the value of SnCu alloys, which is between $0.7\text{--}1.1 \times 10^{-7}\,\Omega\text{m}$ in the case of Sn15Cu – Sn0Cu alloys at room temperature (20 °C) [28].

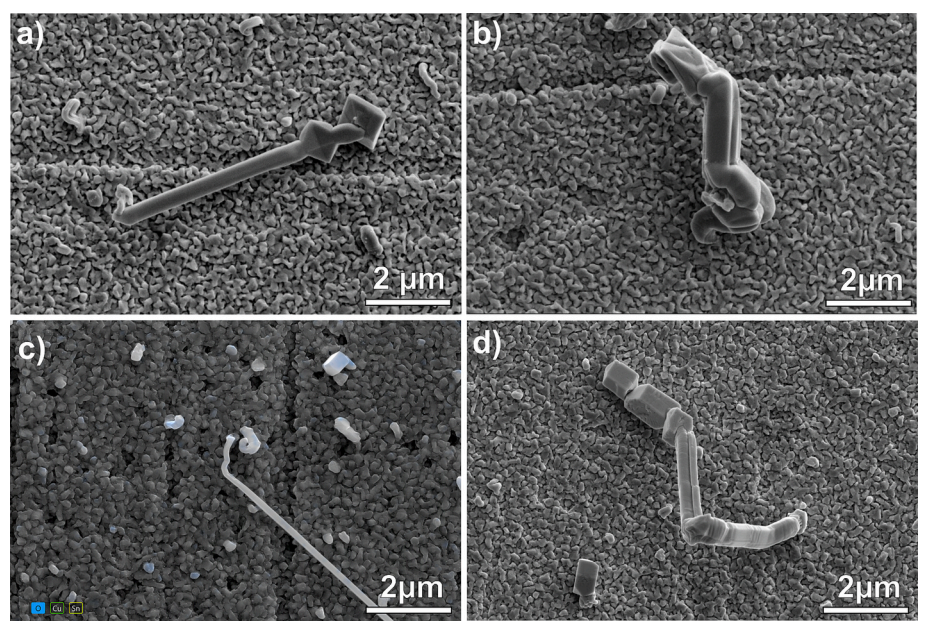


Fig. 3. Sn whiskers on the surface of the PVD Sn layer: a) needle type whisker; b) nodule type whisker; c) 100 nm thick needle type whisker; d) nodule type whisker.

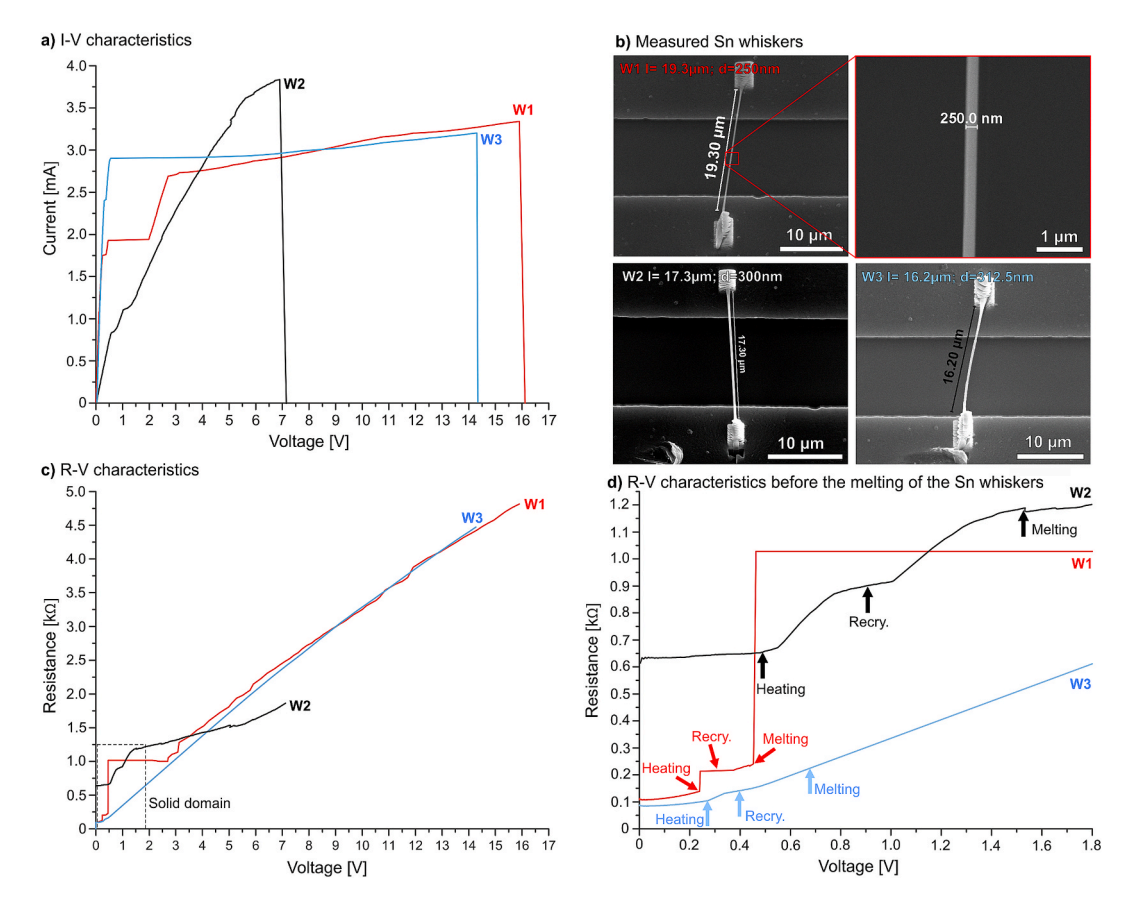


Fig. 4. Electrical characteristics of Sn whiskers measured by the welding method: a) I-V characteristics; b) the measured Sn whiskers; c) resistance–voltage (R-V) diagrams; d) resistance–voltage (R-V) diagrams before the melting of the whiskers.

The cross-section of the whisker is between the ideal circle and the square. Accordingly, minimum and maximum starting electrical resistances can be calculated for the whiskers:

$$R_0 = \rho(T) \cdot \frac{l}{A} \tag{2}$$

where $\rho(T)$ is the specific resistivity $[\Omega m]$, l is the length [m], and A is the surface of the cross-section of the whisker $[m^2]$. Table 1 contains the measured and calculated minimum and maximum values of the electric resistance of the whiskers W1-W3 at room temperature (20 °C). Although the measured resistances are not in the min–max calculated resistance ranges, W1 and W3 are close to them. The differences can be caused by the measurement inaccuracy of the resistance and whisker size measurements, as well as the real specific electrical resistance of the Sn whiskers. In the case of W2 whisker, the difference between the measured and calculated values is considerable. It is likely that the welding of the whisker was not appropriate, resulting in the whisker's connection area to the sample holder being smaller than the whisker's cross-section.

In the solid state, from 20 to 230 °C, the Sn15Cu–Sn0Cu alloys can have 1.75–2.05 times the electrical resistivity increase, reaching $1.4-2.3\times10^{-7}~\Omega m$ [28]. Accordingly, the solid–liquid phase change occurred around 0.4-1.4~V (Fig. 4d). The beginning of the R-V curves

Table 1 Measured and calculated electric resistance values at room temperature (20 $^{\circ}$ C).

Whisker	Measured R_0 [Ω]	Calculated min. R_0 [Ω]	Calculated max. R_0 [Ω]
W1	110	216	433
W2	616	135	269
W3	96	116	233

(between 0 and 1.5 V) has special characteristics: between 0 and 0.25–0.5 V the resistance changes are below 10 %, which means a minor temperature increase of the whisker body. After the temperature starts to increase, the resistance increases are more considerable as well, till the whiskers melt at 0.4–1.4 V. Between the start of the temperature increase and the melting of the whisker, there are characteristic resistance gradient drops after 50–60 % of the resistance increase (Fig. 4d). This might be related to the recrystallization of the Sn whiskers since homogenization causes the electrical resistivity decrease [30,31], which can moderate the temperature-caused resistivity increase. In our case, it occurred around 120–140 °C [28], which is the exact recrystallization temperature range of Sn.

In the liquid state, between 232 and 400 °C, the pure Sn can have a further 2.75 times linear increase in electrical resistivity, reaching $6.3\times10^{-7}~\Omega m$ [28]. Between 400 and 600 °C, the resistivity increase saturates with a further 1.2 times increase, reaching $7.5\times10^{-7}~\Omega m$ [29]. Altogether, Sn can reach a 6.8 times increase in electrical resistivity in the 20–600 °C temperature range. Our whiskers reached 25 times (W1), 3 times (W2), and 20 times (W3), a resistivity increase, which indicated that after the melting, W1 and W3 whiskers must have suffered a decrease in diameter before the fusion. At the first stage of fusion, the molten Sn (with large surface tension) wets the left and right non-molten parts of the whisker, like in the case of any molten fiber, which causes a decrease in diameter.

Fig. 5 presents the electrical characteristics of the first group of Sn whiskers measured by the probing method. The whiskers were named W4–W11. Their physical dimensions were very similar (length 5–25 μ m and diameter 150–350 nm, Fig. 5) to the same parameter of the whiskers measured by the welding method (Fig. 4). The probing method resulted in similar breakdown voltages (6.7–13.8 V, Fig. 5) as the welding method (7.1–16.1 V, Fig. 4), but the current capacities were three orders

A. Skwarek et al. Materials & Design 257 (2025) 114528

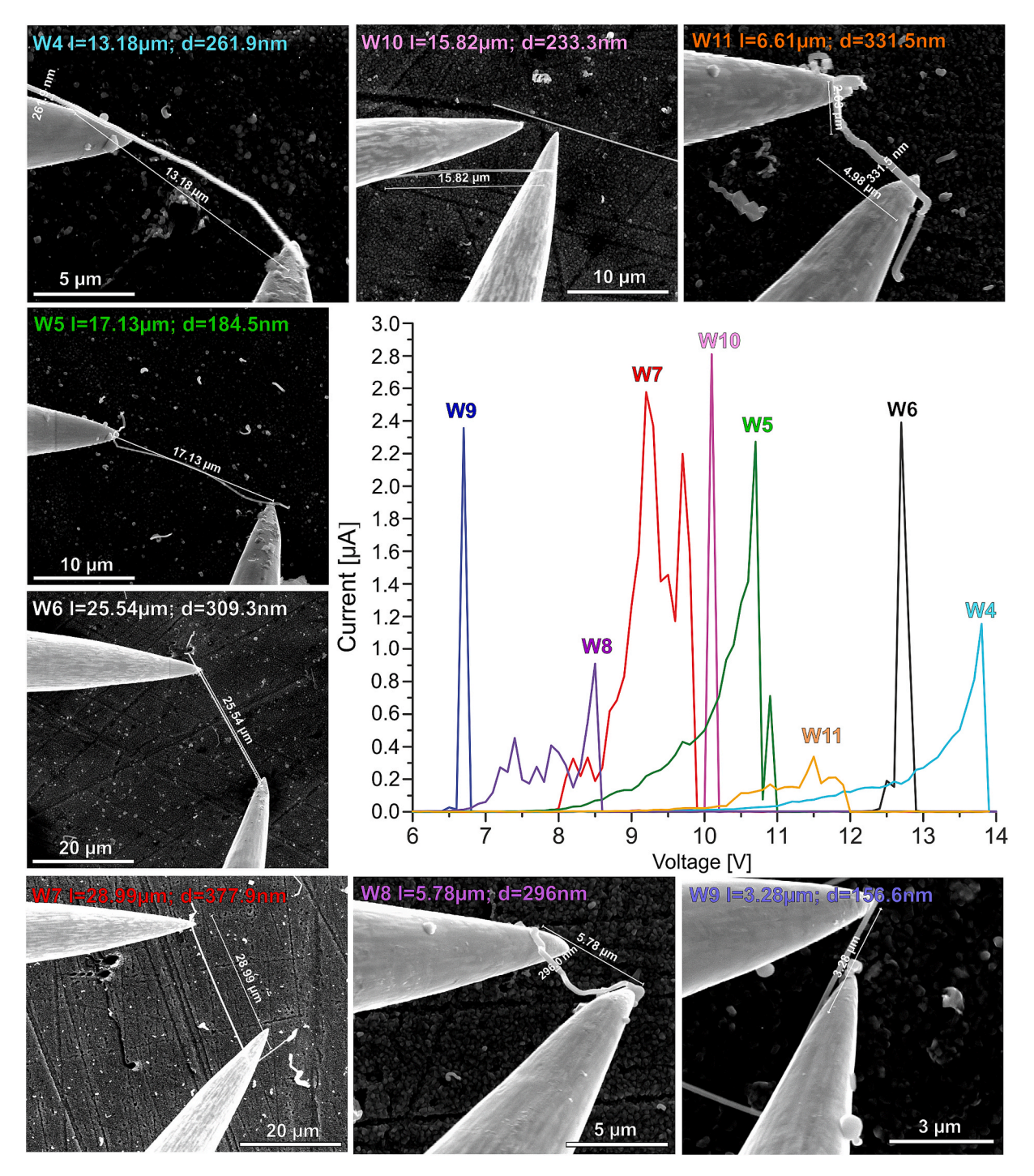


Fig. 5. Sn whiskers measured by the probing method and their I-V characteristics.

of magnitude lower here (0.4–2.8 μ A, Fig. 5) than measured by welding method (3–3.8 mA, Fig. 4). The I-V characteristics differed much during the probing and the welding method. During the probing method, the electric conduction usually starts only at some volts before the breakdown voltage (not from 0 V, like in the case of the welding method). After the whiskers reached the maximum current capacity, they fused. Furthermore, some fluctuations of the I-V values were also typical during the probing method.

The differences between the welding and the probing methods can be explained by the differences in contact resistance and the thermal management effect of the ambient atmosphere. At the welding method, the contact resistance between the probe and the whisker is negligible,

which allows the current flow from very low voltage levels (Fig. 4). At the probing method, the contact resistance can be relatively high, as it was reported by Courey et al. [20,21]. They postulated that the contact resistance contains the oxide film resistance (dominant part) and the constriction resistance, which originates from the roughness of the whisker surface and the possible movement of the whisker during the probing.

The oxide film resistance results in there being no current flow till the oxide film is broken. During the probing method, the oxide layer on the whisker was charged until insulator breakdown occurred. In consequence, I-V characteristics started at low current, and at a certain voltage, they showed a breakdown of the oxide and usually the whole

A. Skwarek et al. Materials & Design 257 (2025) 114528

whiskers. The breakdown could be distinguished into two types: when it was an abrupt breakdown, most visible at W6, W7, W9, and W10 in Fig. 5, and when it was a slower breakdown with a ramp in the current increase, most visible at W1, W4, W5, and W8 in Fig. 5). The type of the breakdown correlated well with the shape of the whisker, abrupt breakdown was typical in the case of the needle type whiskers, while slow breakdown was typical in the case of nodule whiskers. The fluctuation of the I-V curves during the probing method was caused by the construction resistance part of the contact resistance. The considerable current capacity differences between the welding and the probing methods are caused by the thermal management effect of the ambient atmosphere. The heat transfer coefficient decreases considerably with the pressure decrease, at 30kPA 40-50 % [32], and 10 kPa 90 % [33] of decrease was reported. This effect of vacuum on the heat transfer is applied in vacuum insulated tubing (VIT) technology [34] or in vacuum tube transportation (VTT) systems [33]. So, during the welding method measurements, the ambient air can cool the surface of the Sn whiskers by natural convection heat transfer, and they can conduct three orders of magnitude larger currents than during the probing method in a vacuum.

Fig. 6 presents the electrical characteristics of the second group of Sn whiskers (W12 – W16) measured by the probing method. Their diameter was thicker (300–800 nm, Fig. 6) than measured previously (150–350 nm, Fig. 5). Consequently, the detected current capacities were also generally larger, between 4.5 and 11.5 μA , as it was predictable from Eq. (2). The breakdown voltages did not change, 5.8–12.2 V. Here, W15 was a typical needle-type whisker, which showed an abrupt breakdown, while W12–W14 whiskers were typical nodule whiskers, which showed a slow breakdown (Fig. 6). As the I-V characteristics depend on the breaking of the oxide layer on the surface of the whiskers, the oxidation state of the different type of the whiskers must have differed.

Fig. 7 presents two examples (whiskers W12 and W15) of the effect of the probing measurement on the whiskers. The left side of Fig. 7 shows the whiskers before the measurement, and the right side shows them after the fusion. The large surface tension in the vacuum formed Sn balls

from the whiskers, which either stuck to one of the probes or dispersed on the surface of the sample.

Fig. 8 summarizes the electrical parameters (current capacity (Fig. 8a) and breakdown voltage (Fig. 8b)) of the 20 pieces of Sn whiskers, 10-10 nodule- and needle-type, measured by the probing method. The diameter of the tested whiskers was between 0.15 and 4.5 μ m, so a logarithmic scale was used on the x-axis. The current capacities (Fig. 8a) were detected over a wide range as well (0.001–100 mA), so a logarithmic scale was justified on the y-axis of Fig. 8a as well. Whiskers having a diameter below 1 μ m have a low current capacity, typically between 1 and 10μ A. In contrast, thicker whiskers having a diameter above 3 μ m have a three-order-of-magnitude higher current capacity, between 10 and 100 mA. In the case of the red-marked points 2 and 3 in Fig. 8a, the fusion did not happen; the whiskers could survive the current limit of the measurement device (100 mA).

Comparing the measured current capacities to data from the literature [23,24], in the case of thicker Sn whiskers (typically nodule-type whiskers with $d>0.5~\mu m$), the results agree well. There is no information in the literature about the current capacity of whiskers having diameters under 0.5 μm , which are typically needle-type. The breakdown voltages do not show a correlation with the diameter of the Sn whiskers (Fig. 8b). The Same results were presented in [19] and [20]. As discussed above, the breakdown voltage is determined by the contact resistance between the whisker and the probe and not by the diameter of the whisker. The average breakdown voltage was $10.28\pm4.84~V$. Previously, Han et al. [19] observed 7.57 V, and Courey et al. [20] observed 11.8 V on average, which matches the results of this study well. In the case of the red-marked point (1) in Fig. 8b, the fusion did not happen; the voltage limit of the measurement device (40 V) could not generate enough high currents for the fusion.

Table 2 summarizes the averages of the electrical parameters as a function of the measurement method and the type of whisker. In the case of needle-type Sn whiskers, the three orders of magnitude differences in the current capacities between the welding and the probing methods

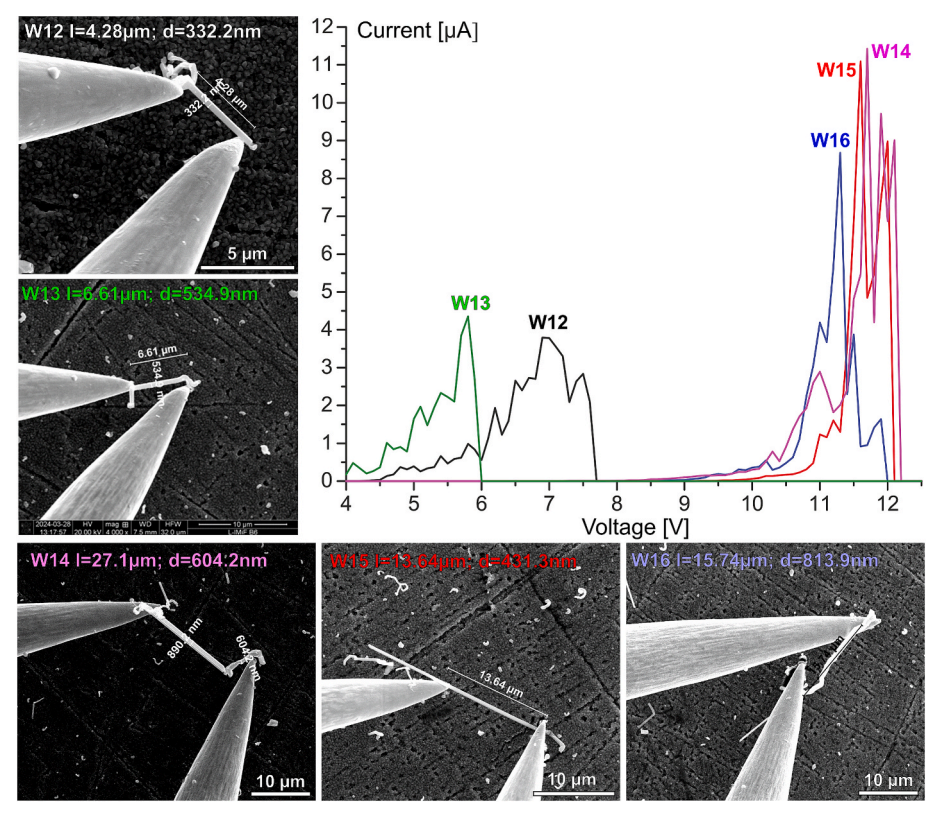


Fig. 6. I-V characteristics of Sn whiskers measured by the probing method.

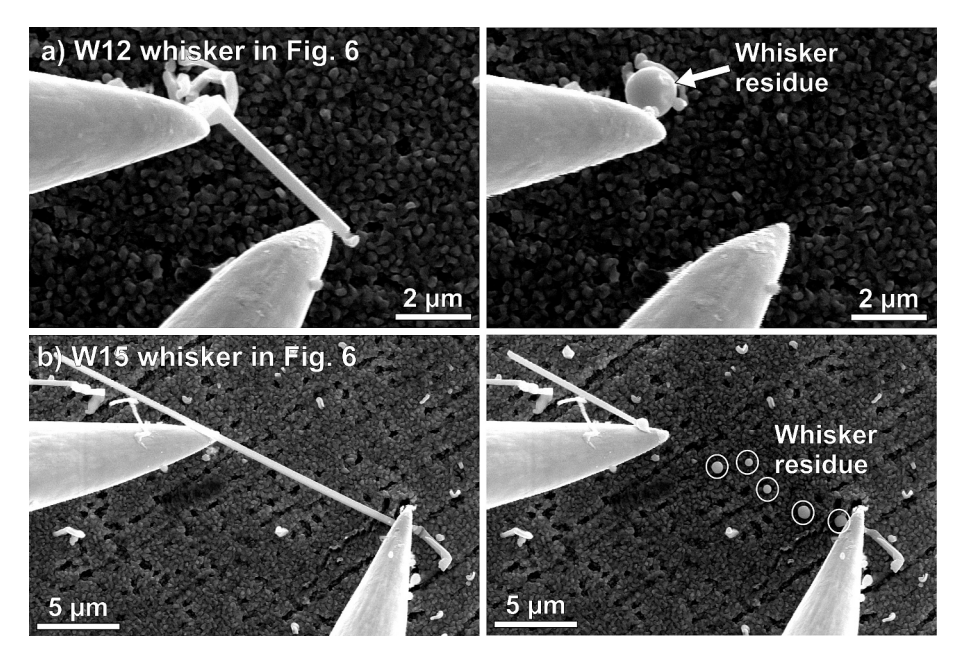


Fig. 7. Whiskers before (left) and after (right) the probing measurement: a) W12 whisker in Fig. 6; b) W15 whisker in Fig. 6.

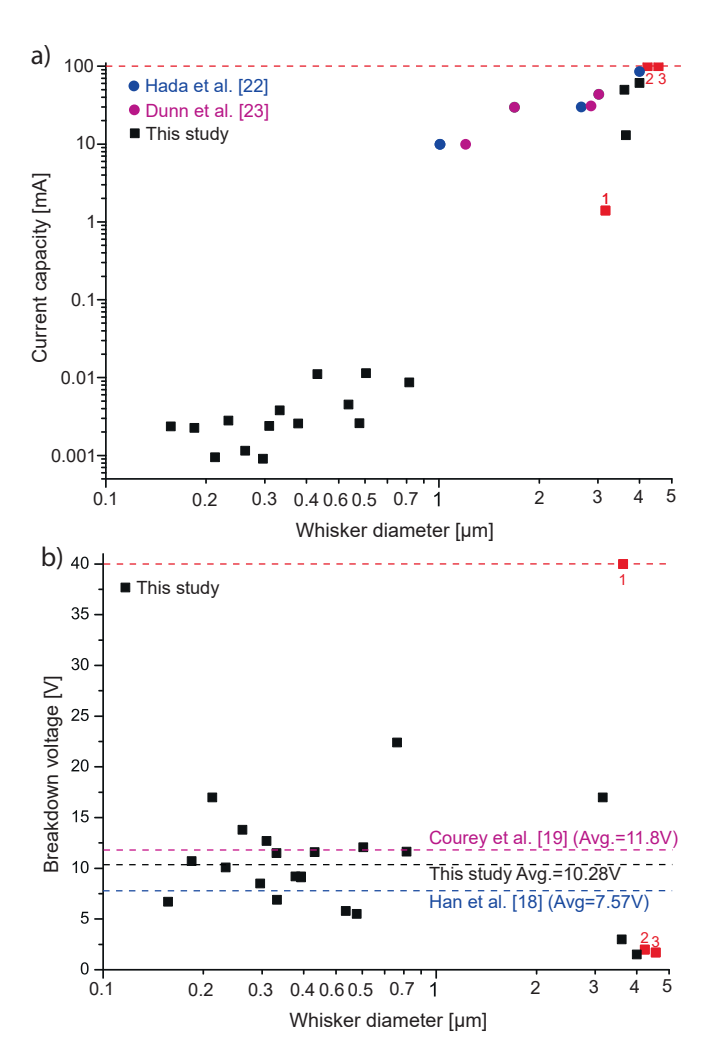


Fig. 8. Electrical parameters of the Sn whiskers in function of the whisker diameter, measured by the probing method: a) current capacity; b) breakdown voltage.

could be explained by the thermal management effect of the ambient air during the welding method, as discussed above.

In the case of the probing method, the diameter of the whisker changed in a wide range (between $0.15~\mu m$ and $4.5~\mu m$), but their length was in a narrower range between 6 and 40 μm , with a 16.8 μm average. So, the current capacity of the whiskers was determined mainly by the square of the whisker diameter (Eq. (2). On average, the nodule-type whiskers were 10 times thicker than the needle-type whiskers; thus, they should be able to conduct 100 times higher currents. In this study, considerably higher, on average, 166 times current capacity increase was observed in the case of nodule-type whiskers. In addition, their I-V characteristics also differed during the breakdown, so further investigations were done.

The oxidation state of the different types of whiskers was compared using EDS measurements. The average atomic percentage of oxygen on the surface of the needle-type whiskers was 4.9 ± 0.6 at%, while on the surface of the nodule-type whiskers it was 7.5 ± 0.8 at%. The 53% thicker oxide layer on the surface of the nodule-type whiskers could explain their slower breakdown (Figs. 5 and 6), since the thicker oxide layer means larger capacity, which takes more time to charge by the current and reach the insulator breakdown. However, it does not explain the larger current capacity of the nodule-type whisker (Tab. 2); furthermore, the reason for the different oxidation levels in the case of the different whisker types is still unclear. TEM lamellae were fabricated from a needle and a nodule type of whiskers to investigate the above-discussed issues further. The results of the TEM investigations are presented in Fig. 9.

Fig. 9a shows the TEM micrograph of the end of a needle whisker. The body of the whisker was marked by a red line. The block-like structure, a characteristic feature of the vacuum-grown whiskers, is well observable. The body of the whiskers contained inclusions, as it was reported by Illés et al. [28]. A large one, with 50 nm diameter, is presented on the HR TEM micrograph in Fig. 9b. The whisker monocrystalline, and the same SAED results presented in Fig. 9c were measured at several points in the body of the whisker. The Sn matrix had (220) and (101) orientations, which is the most typical for the Sn. The EDS measurements (Fig. 9d) proved that the inclusion contained a large amount of Cu (40 at%). The atomic ratio of Sn/Cu was very close to the composition of Cu₆Sn₅ (56/44 at% to Sn/Cu). Similar results were reported by Illés et al. [27], where they postulated that the Cu/Cu₆Sn₅ were taken by the interface flow mechanism into the whisker body. The

Table 2 Electrical parameters in the function of the measurement method and the type of the whisker.

Welding needle 0.15–0.5 – 12.5 3.5 Probing needle 0.15–0.5 abrupt 11.2 0.003	Measurement	Whisker type	Whisker diameter [µm]	Breakdown type (I-V char.)	Avg. breakdown voltage [V]	Avg. current capacity [mA]
Probing nodule 0.5-4.5 slow* 10.1 0.5	Probing	needle	0.15-0.5	abrupt	11.2	0.003

^{*}When the current (100 mA) or the voltage (40 V) limit of the measurement device was reached, the fusion did not happen.

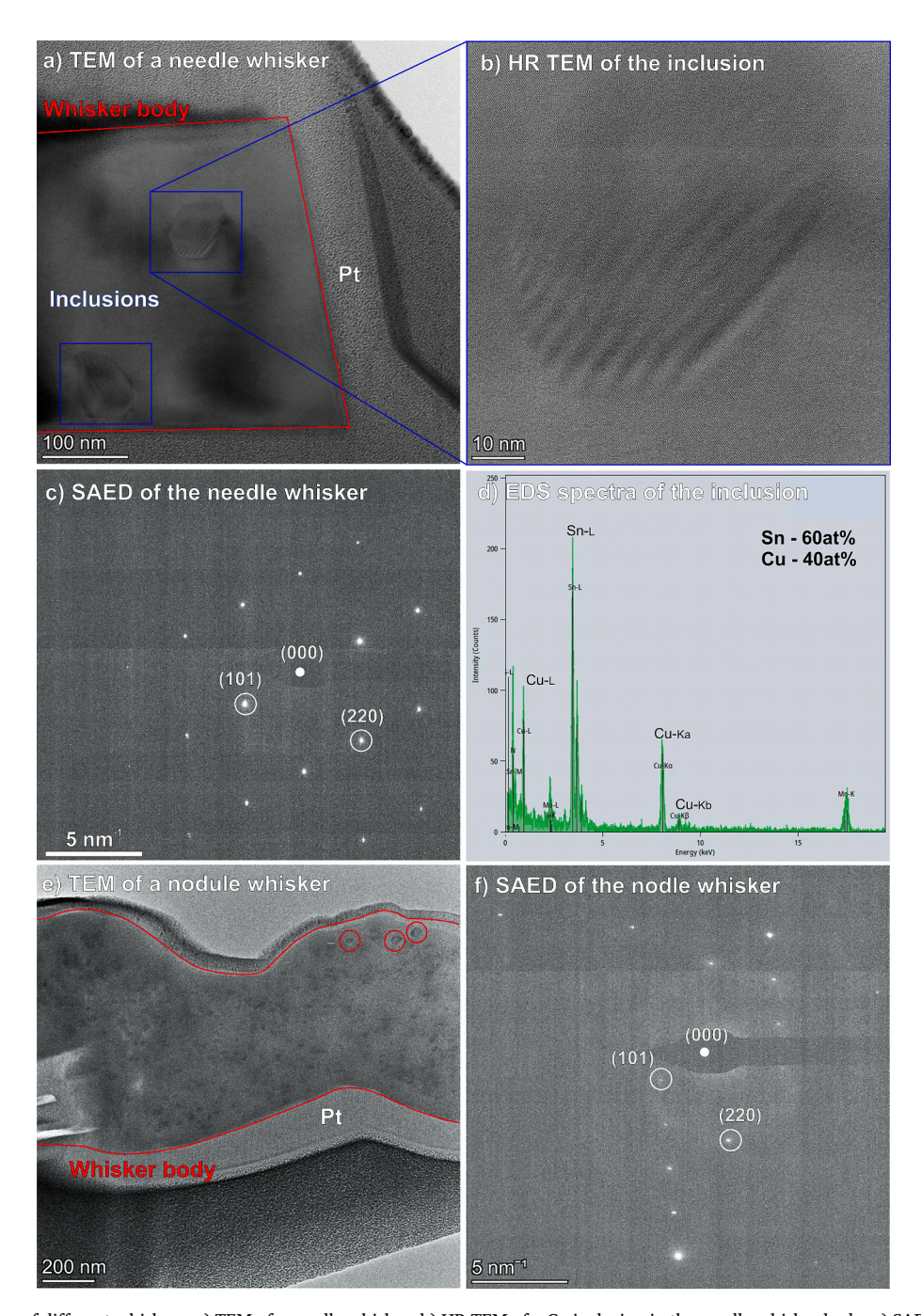


Fig. 9. TEM investigation of different whiskers: a) TEM of a needle whisker; b) HR TEM of a Cu inclusion in the needle whisker body; c) SAED of the needle whisker; d) EDS spectra of the needle whisker; e) TEM of a nodule whisker; f) SAED of the nodule whisker.

 Cu_6Sn_5 IMC layer growth indicates such a large stress in the thin Sn layer that could initiate the interface flow mechanism, which means the flow of Sn and Cu (or Cu_6Sn_5) atoms (or molecules) along a fluid-like viscous layer at the interface of the Sn film and the Cu_6Sn_5 IMC layer [27].

Fig. 9e shows the TEM micrograph of a nodule-type whisker. The

body of the whisker was marked by a red line. According to the contrast differences, this whisker contains plenty of Cu inclusions as well; some of them are marked by red circles in Fig. 9e. The Cu inclusions were distributed evenly in the body of the whiskers, as it is well observable in Fig. 9e (darker spots in the whisker body), in the case of the needle-type

whisker as well. The SAED measurements in Fig. 9f proved that the nodule-type whisker is also monocrystalline with the same orientations (220) and (101), as the needle-type in Fig. 9c. No major differences were found between the microstructures of the needle- and nodule-type whiskers; however, the nodule-type whisker contained twice as many Cu inclusions (10.9 at%) as the needle-type (4.5 at%). A former study found a similar difference between the nodule- and needle-type whiskers, namely nodule-type whiskers contained 8–12 at% Cu/Cu₆Sn₅ inclusions and the needle-type only 4–5 at% [27].

The larger amount of Cu in the nodule-type whiskers decreases their electrical resistivity, but not to the extent that would explain their 66 % larger current capacity compared to the needle-type whiskers (Tab. 2). In the given range of Cu content (5–11 at%), the electrical resistivity decreases only around 20 % [28]. The remaining 30–46 % current capacity increase could be related to the better thermal properties of the nodule-type whiskers due to their larger diameter. Supposed to be no considerable temperature gradient in the whisker during the probing electrical characterization, they could lose heat only by radiation. The radiated heat is directly proportional to the surface of the radiating object, which is proportional to the square of the whiskers' diameter. In addition, the thermal capacity of the whisker is proportional to the third power of the diameter. Consequently, the increase in diameter can many times improve the thermal management of the whiskers.

The main conclusions of the study are that inside a spacecraft (under ambient conditions), with the thermal management effect of the atmosphere, any whisker can cause a serious reliability risk. As we observed, thicker Sn whiskers can conduct over 100 mA current without fusion, already at 1.5 V breakdown voltage. Modern microcontrollers typically operate with a minimum logic high voltage ranging from 2.0 V to 3.3 V, which is far over the lowest breakdown voltage obtained in this study (1.5 V). The 100 mA current is far enough to operate a 0.25 W LED, and even 5–10 mA of short-circuit current can cause logical failure in a microcontroller. In the part of the spacecraft under vacuum conditions, the reliability risk is lower. First of all, shorter and thinner whiskers grow in vacuum circumstances than in ambient [27]; and second, smaller currents can form since the whiskers fuse over some mA of current, but the conduction starts from 0 V voltage since there is no oxide layer on the surface of the whisker.

4. Conclusions

The electrical parameters of thermal vacuum grown Sn whiskers were investigated. Two measurement methods were applied; the first measured the pure electrical parameters in ambient conditions by welding the whisker to a sample holder; the second was the classical probing method in vacuum, which simulated the real circumstances when a whisker touched a conductive surface. The main findings are the following:

- The measured electrical resistance of the Sn whiskers was close to the
 calculated theoretical values. The average breakdown voltage was
 10–12 V, in both measurements and in the case of any type of
 whiskers, which fits well with the literature. In contrast, the current
 capacity depends considerably on the measurement circumstance
 and the type of whisker used.
- Two types of I-V characteristics of the whisker were observed: an abrupt breakdown in the case of needle-type whiskers and a slower breakdown with a ramp in the current increase in the case of noduletype whiskers. Furthermore, nodule-type whiskers had a relatively larger current capacity than needle-type whiskers.
- TEM investigations did not show considerable microstructural differences between the nodule- and needle-type whiskers. Both were mono-crystalline with the same orientations. However, nodule-type whiskers were more oxidized and contained more Cu/Cu₆Sn₅ inclusion than the needle-type whiskers. These microstructural

differences explain the differences between the I-V characteristics and the conductivities.

- In ambient conditions, the whisker can conduct more than three
 orders of magnitude larger current than in a vacuum due to the
 thermal management effect of the ambient air. Inside a spacecraft,
 any whisker can cause serious reliability risks. In this study, 100 mA
 current was measured without the fusion of the whisker.
- The space industry can use the obtained electrical parameters for risk analyses and the development of short-circuit protection systems. In the future, we plan to investigate further the relation between the type of whiskers and their electrical parameters in terms of the observed microstructural differences.

CRediT authorship contribution statement

Agata Skwarek: Writing – review & editing, Supervision, Resources, Project administration, Formal analysis, Conceptualization. Balázs Illés: Writing – original draft, Visualization, Validation, Supervision, Methodology. Ernest Brzozowski: Visualization, Validation, Investigation, Formal analysis, Data curation, Conceptualization. Adam Laszcz: Software, Methodology, Investigation, Formal analysis, Data curation. Piotr Zachariasz: Validation, Software, Investigation, Formal analysis, Conceptualization.

Declaration of competing interest

The authors declare that they have no known competing financial interests or personal relationships that could have appeared to influence the work reported in this paper.

Acknowledgment

This work was carried out under a program of and funded by the European Space Agency, entitled "Current Capacity and Effects of Vacuum of Tin Whiskers", ESA AO/1-11458/22/NL/FE. The authors acknowledge the support of M. Lekka and P. López (CIDETEC) in providing the Cu substrates and of B. Pécz and L. Illés (HUN-REN) in preparing the TEM specimen. B.I. and A.S. acknowledge the support of the National Science Center Poland (NCN) project no. 2022/47/B/ST5/00997. The view expressed herein can in no way be taken to reflect the official opinion of the European Space Agency.

Data availability

The raw/processed data required to reproduce these findings cannot be shared at this time as the data also forms part of an ongoing study.

References

- L. Tersztyánszky, B. Illés, Incompatibility Problems in Soldering Technology, Proceedings of 28th IEEE-ISSE conference 2005, pp. 90-96. doi: 10.1109/ ISSE.2005.1491009.
- B.D. Dunn, Guidelines for creating a leadfree control plan, technical report, 2012,
 42 p. https://esamultimedia.esa.int/multimedia/publications/STM-281/STM-281.
 pdf, 2012 (accessed 29 May 2025).
- [3] ESA, Roadmap for Lead-free Transition in the European Space Sector, technical report, 2020, 24 p. https://escies.org/download/webDocumentFile?id=70002, 2020 (accessed 29 May 2025).
- [4] A. Coello-Vera, G. Corocher, Pb-free Transition for the European Space Sector, Presentation on ESCCON conference, online, March 9–11, 2021. https://escies.org/download/webDocumentFile?id=68426, 2021, (accessed 29 May 2025).
- [5] B.Z. Lee, D.N. Lee, Spontaneous growth mechanism of tin whiskers, Acta Mater. 46 (June 1998) 3701–3714, https://doi.org/10.1016/S1359-6454(98)00045-7.
- [6] J. Richardson, B. Lasley, Tin Whisker Initiated Vacuum Metal Arcing in Spacecraft Electronics, in Proc. of 18th Government Microcircuit Applications Conference, November 10–12, 1992, pp. 119–122.
- [7] D. Van Westerhuyzen, P. Backes, J. Linder, S. Merrell, R. Poeschel, Tin Whisker Induced Failure In Vacuum, in Proc. of 18th International Symposium for Testing & Failure Analysis, October 17, 1992, pp. 407–412.
- [8] M. Umalas, S. Vlassov, B. Polyakov, L.M. Dorogin, R. Saar, I. Kink, R. Löhmus, A. Löhmus, A.E. Romanov, Electron beam induced growth of silver nanowhiskers,

- J. Cryst. Growth 410 (January 2015) 63–68, https://doi.org/10.1016/j.icrysgro.2014.10.021.
- [9] J. Brusse, Tin whiskers: Revisiting an old problem, EEE Links 4 (4) (1998) 5-7.
- [10] J.A. Brusse, G.J. Ewell, J.P. Siplon, Tin Whiskers: Attributes and Mitigation, in Proc. of 22nd Capacitor and Resistor Technology Symposium, New Orleans, March 25-29, 2002, pp. 67-80. https://nepp.nasa.gov/whisker%20/reference/tech_ papers/brusse2002-paper-tin-whiskers-attributes-and-mitigation-CARTS-europe. pdf (accessed 29 May 2025).
- [11] J.J. Williams, N.C. Chapman, N. Chawla, Mechanisms of Sn hillock growth in vacuum by in situ nanoindentation in a scanning electron microscope (SEM), J. Electron. Mater. 42 (February 2013) 224–229, https://doi.org/10.1007/s11664-012-2209-0.
- [12] K.-W. Moon, C.E. Johnson, M.E. Williams, O. Kongstein, G.R. Stafford, C. A. Handwerker, W.J. Boettinger, Observed correlation of Sn oxide film to Sn whisker growth, J. Electron. Mater. 34 (May 2005) L31–L33, https://doi.org/ 10.1007/s11664-005-0274-3.
- [13] M.W. Barsoum, E.N. Hoffman, R.D. Doherty, S. Gupta, A. Zavaliangos, Driving force and mechanism for spontaneous metal whisker formation, Phys. Rev. Lett. 93 (November 2004) 206104, https://doi.org/10.1103/PhysRevLett.93.206104.
- [14] K. Suganuma, A. Baated, K.S. Kim, K. Hamasaki, N. Nemoto, T. Nakagawa, T. Yamada, Sn whisker growth during thermal cycling, Acta Mater. 59 (November 2011) 7255–7267, https://doi.org/10.1016/j.actamat.2011.08.017.
- [15] S. Ichimaru, H. Tatsumi, T. Nakagawa, H. Nishikawa, Study of the characteristics and growth of tin whiskers in orbit, Microelectron. Reliab. 162 (November 2024) 115523, https://doi.org/10.1016/j.microrel.2024.115523.
- [16] J.L. Jo, S. Nagao, T. Sugahara, M. Tsujimoto, K. Suganuma, Thermal stress driven Sn whisker growth: in air and in vacuum, J. Mater. Sci. Mater. Electron. 24 (June 2013) 3897–3904, https://doi.org/10.1007/s10854-013-1336-6.
- [17] O. Oudat, V. Arora, E.I. Parsai, V.G. Karpov, D. Shvydka, Gamma- and x-ray accelerated tin whisker development, J. Phys. D Appl. Phys. 53 (October 2020) 495305, https://doi.org/10.1088/1361-6463/abb38d.
- [18] Y. Liu, P. Zhang, J. Yu, J. Chen, Y. Zhang, Z. Sun, Confining effect of oxide film on tin whisker growth, J. Mater. Sci. Tech. 35 (August 2019) 1735–1739, https://doi. org/10.1016/j.jmst.2019.03.042.
- [19] S. Han, M. Osterman, M.G. Pecht, Electrical shorting propensity of tin whiskers, IEEE Trans. Electron. Pack. Manuf. 33 (July 2010) 205–211, https://doi.org/ 10.1109/TEPM.2010.2053377.
- [20] K.J. Courey, S.S. Asfour, A. Onar, J.A. Bayliss, L.L. Ludwig, M.C. Wright, Tin whisker electrical short circuit characteristics—Part II, IEEE Trans. Electron. Pack. Manuf. 32 (January 2009) 41–48, https://doi.org/10.1109/TEPM.2008.2009224.
- [21] K.J. Courey, S.S. Asfour, J.A. Bayliss, L.L. Ludwig, M.C. Zapata, Tin whisker electrical short circuit characteristics—Part I, IEEE Trans. Electron. Pack. Manuf. 31 (January 2008) 32–40, https://doi.org/10.1109/TEPM.2007.914210.

- [22] N.A.J. Sabbagh, H.J. McQueen, Tin whiskers: Causes and remedies, Met. Finish. 73 (1975) 27–31.
- [23] Y Hada, O Morikawa, H Togami, Study of tin whiskers on electromagnetic relay parts, in Proc. 26th Relay Conference, Apr. 25–26 (1978) 1–9.
- [24] B.D. Dunn, Mechanical and electrical characteristics of tin whiskers with special reference to spacecraft systems, ESA Journal, 12 (1988) 1-17. https://nepp.nasa. gov/whisker/reference/tech_papers/dunn1988-mechanical-and-electricalcharacteristics-of-tin-whiskers.pdf (accessed 29 May 2025).
- [25] L. Panashchenko, The Art of Appreciating Metal Whiskers: A Practical Guide for Electronics Professionals, in Proc. of IPC Tin Whisker Symposium, Dallas, TX, 2012. https://nepp.nasa.gov/whisker/reference/tech_papers/2012-Panashchenko-IPC-Art-of-Metal-Whisker-Appreciation.pdf (accessed 29 May 2025).
- [26] M.S. Mason, G. Eng, Understanding tin plasmas in vacuum: A new approach to tin whisker risk assessment, J. Vac. Sci. Tech. A 25 (2007) 1562–1566, https://doi. org/10.1116/1.2796181.
- [27] B. Illés, A. Skwarek, T. Hurtony, O. Krammer, B. Medgyes, K. Szostak, G. Harsányi, A. Kovács, B. Pécz, Risk of transition to lead-free in the space sector – Sn whisker growth in thermal vacuum conditions from submicron Sn layer, Mater. Des. 250 (February 2025) 113637, https://doi.org/10.1016/j.matdes.2025.113637.
- [28] E. Cadırl, H. Kaya The effect of composition on microhardness and determination of electrical and thermal properties in the Sn-Cu alloys, J. Mater. Sci.: Mater. Electron. 22 (February 2011) 1378–1386. DOI 10.1007/s10854-011-0317-x.
- [29] M. Pokorny, H.U. Astrom, Temperature dependence of the electrical resistivity of liquid tin between 214°C and 705°C, J. Phys. F: Metal Phys. 5 (1975) 1327, https://doi.org/10.1088/0305-4608/5/7/012.
- [30] A.R. Eivani, H. Ahmed, J. Zhou, J. Duszczyk, Correlation between electrical resistivity, particle dissolution, precipitation of dispersoids, and recrystallization behavior of AA7020 aluminum alloy, Metal. Mater. Trans. A 40 (October 2009) 2435–2446, https://doi.org/10.1007/s11661-009-9917-y.
- [31] J. Freudenberger, A. Kauffmann, H. Klauß, T. Marr, K. Nenkov, V. Subramanya Sarma, L. Schultz, Studies on recrystallization of single-phase copper alloys by resistance measurements, Acta Mater. 58 (April 2010) 2324–2329, https://doi.org/ 10.1016/j.actamat.2009.12.018.
- [32] J. Mir-Bel, R. Oria, M.L. Salvador, Influence of temperature on heat transfer coefficient during moderate vacuum deep-fat frying, J. Food Eng. 113 (November 2012) 167–176, https://doi.org/10.1016/j.jfoodeng.2012.06.009.
- [33] Y. Mao, M. Yang, T. Wang, F. Wu, B. Qian, Influence of vacuum level on heat transfer characteristics of maglev levitation electromagnet module, Appl. Sci. 10 (February 2020) 1106, https://doi.org/10.3390/app10031106.
- [34] J. H. Azzola, P. D. Pattillo, J. F. Richey, S. J. Segreto, The Heat Transfer Characteristics of Vacuum Insulated Tubing, in Proc. of SPE Annual Technical Conference and Exhibition, Houston, Texas, September 26–29, 2004, SPE 90151. doi: 10.2118/90151-MS.